Influence of fabrication parameters on crystallization, microstructure, and surface composition of NbN thin films deposited by rf magnetron sputtering

J. E. Alfonso · J. Buitrago · J. Torres ·
J. F. Marco · B. Santos

Abstract In this work NbN thin films have been grown by magnetron rf sputtering of a δ-NbN (99.99%) target. In particular, the influence of certain fabrication parameters (substrate temperature, power supplied to the target or additional N_2 flux in the preparation chamber) on the crystallization, microstructure, and surface composition of the deposited films have been studied. The films have been characterized by X-ray diffraction (XRD) at grazing angle in the θ–2θ configuration, scanning electron microscopy (SEM), wavelength dispersive spectrometry (WDS), and X-ray photoelectron spectroscopy (XPS). XRD results show that films grown at a substrate temperature of 573 K and a power supply applied to the target of 300 W present the same crystalline structure of the target while films grown at these temperature and power supply conditions plus the additional presence of N_2 during fabrication, grow highly textured along the plane (200). SEM results indicate that the films present columnar growth and a high homogeneity. WDS analysis shows that films grown at 573 K and 300 W are stoichiometric. XPS shows a complex surface composition of the films most external 5 nm,

indicating the presence of niobium nitride (NbN_x), niobium oxy-nitride (NbN_xO_y), and niobium oxide (Nb_2O_5).

Introduction

Due to their mechanical properties, their high fusion points and thermal and chemical stability, transition metal nitrides present a great variety of applications spanning from hard coatings to electromagnetic radiation detectors. In particular, NbN has been studied as a potentially useful material for low temperature electronics, for instance, multilayer films of the type (NbN/AlN/NbN) have been used as tunnel junctions [1, 2]. Likewise, the possibility of using NbN as cathode in vacuum microelectronic devices has been considered [3]. Other nitrides such as TiN and TaN have been used as diffusion barriers to prevent copper diffusion into silicon. Finally, the characterization of the mechanical properties of AlN and CrAlN thin films is a matter that has received recently considerable attention [4, 5].

Although NbN has been prepared as thin films using different techniques including reactive phase rf magnetron sputtering [6, 7], pulsed laser deposition (PLD), or atomic layer deposition [8], the influence that some deposit fabrication parameters such as argon pressure in the work chamber or the power supplied to the target has on the structural properties of the materials deposited has not been investigated in depth. This work presents results obtained from the growth of NbN thin films on glass substrates, through rf magnetron sputtering technique which has proven to be quite versatile to prepare a variety of different materials [9–11]. In particular, we have studied the influence of certain fabrication parameters (substrate temperature, power supplied to the target and additional N_2 flux in the preparation chamber) on the

J. E. Alfonso (✉) · J. Buitrago · J. Torres
Grupo de Materiales con Aplicaciones Tecnológicas,
Universidad Nacional de Colombia, A.A. 14490 Bogotá, DC,
Colombia
e-mail: jealfonsoo@unal.edu.co

J. F. Marco · B. Santos
Instituto de Química-Física "Rocasolano" CSIC, c/Serrano, 119,
28006 Madrid, Spain

B. Santos
Universidad Autónoma de Madrid, Madrid, Spain

crystallization, microstructure, and surface composition of the deposited films.

Experimental techniques

The equipment used to grow the NbN films is an Alcatel HS 2000 described in previous papers [12]. The NbN films were obtained from a $4'' \times 1/4''$ NbN (99.9%) target (CERAC, Inc.). The parameter set used during deposition process was: base pressure (2.0×10^{-4} Pa), total working pressure (7×10^{-1} Pa), deposition time (half an hour), target–substrate distance (5 cm), argon (99.999%) flux (20 sccm). Under these experimental conditions the deposition rate was estimated to be 20 nm min^{-1}. We studied the influence of several deposition parameters such as: power supplied to the target, substrate temperature, which varied from 513 to 573 K, and additional nitrogen (99.99%) flux inside the deposit chamber (2, 4, and 6 sccm). The final working pressure was maintained using a valve controller for all the nitrogen flow values given above, the temperature of the substrate was measured with thermocouple type K and the argon and nitrogen flows were controlled with mass flow controllers.

The structural characterization of the films was performed by X-ray diffraction (XRD) with a Philips diffractometer operated at 30 kV and 20 mA and using Cu Kα radiation. The grain size was calculated from $\tau = 0.9\lambda/B\cos\theta$ where $B = B_m^2 - B_i^2$, being B the broadening of the diffraction line, B_m the measured full width at half maximum (FWHM) and B_i the instrument peak width. Surface morphology was characterized by imaging the secondary electrons with a Quanta 2000 scanning electron microscope operating at 15 kV and 10 mA. Chemical composition was evaluated by wavelength dispersive spectrometry (WDS) using a Jeol 5910 LV scanning electron microscope operated at 13 kV. The surface chemical composition was determined by X-ray photoelectron spectroscopy (XPS) using a Leybold-Heraeus LHS-10 spectrometer under a vacuum better than 3×10^{-8} Pa using Mg Kα radiation (1254.6 eV) and a constant pass energy of 20 eV. Binding energies were referred to the C1s line (284.6 eV) of the adventitious contamination layer.

Results and discussion

XRD data recorded from the niobium nitride target used confirmed its δ-NbN structure with a lattice parameter of $a = 4.3927$ Å.

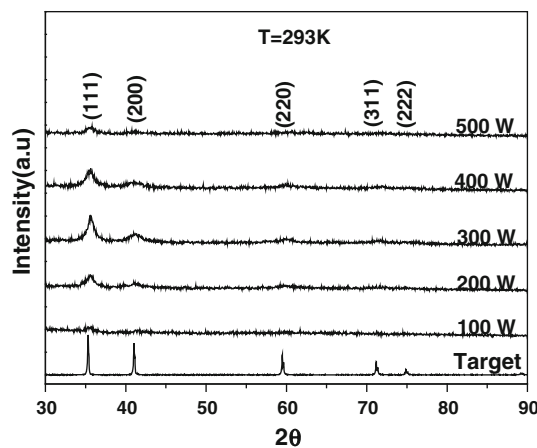Figure 1 shows the XRD patterns recorded from the films grown at room temperature and different power

Fig. 1 XRD patterns recorded from NbN films deposited at 293 K and different power supplies applied to the target

supply values applied to the target. In general, the data recorded from all the samples showed quite broad diffraction lines what is an indication of the poor crystallinity of the films grown. This is particularly true for the films grown at target powers lower than 200 W. Although still showing broad lines, the films grown at powers in the range 200–400 W present more intense lines than the latter showing a polycrystalline structure that reproduces that of the target. It is important to note (Fig. 1) that the films grown at 500 W appear to be of a lesser crystallinity than those grown at 300 W. This behavior can be explained by effects of re-sputtering that occur at high powers of deposit. Our results are in agreement with previous work [13] in which it was established that 300 W is an optimum power to deposit NbN thin films.

Figure 2 shows the XRD patterns corresponding to the films grown at 300 W and different substrate temperatures. The NbN target pattern has been included as a reference. In general, the patterns recorded from the different grown films present the same reflections than the target, i.e., those of the δ-NbN cubic phase, but showing important differences on the relative intensities, in particular, those corresponding to planes (111) and (200) which increase with increasing temperature. Regarding this, it is important to point out that, contrary to what occurs in the target and rest of film patterns, the diffraction pattern of the film grown at 553 K shows a larger intensity for the reflection from plane (111) than from that corresponding to the plane (200). While the (111) line in the target pattern has a relative intensity of 100% compared to 86% of line (200), in the 553 K sample the relative intensity of the (200) line is, approximately, 6% of the corresponding (111) line. The result indicates that the supply of additional 22.4 meV to the substrate (which is the energy difference between room temperature and 553 K) does not bring about changes in the polycrystalline character of the materials, but gives
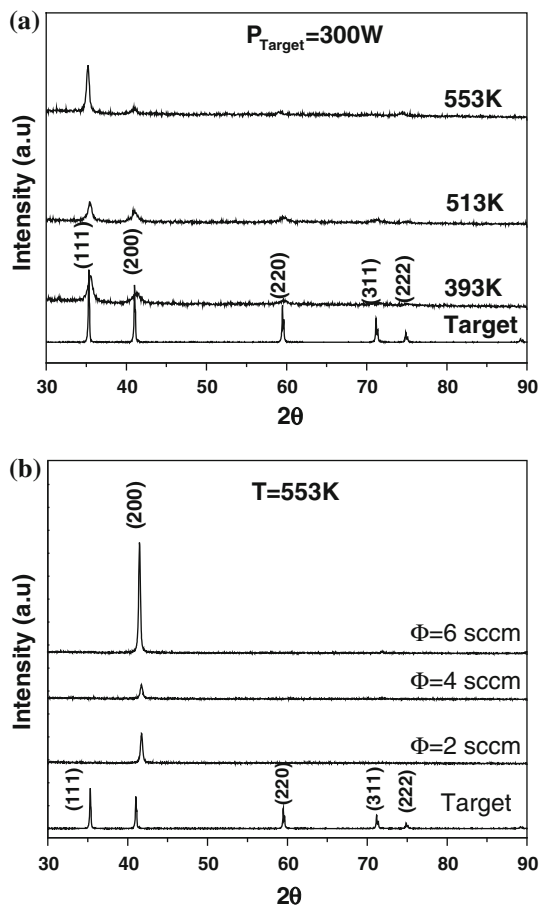
Fig. 2 XRD patterns recorded from NbN films deposited at **a** 300 W and different temperatures and **b** 553 K, 300 W and different nitrogen fluxes. The pattern of the target from which the films were obtained is included for comparison purposes

place to the growth of films with preferred orientation along the (111) plane. There are similarities between the work presented here and recent reports on the characterization of NbN thin coatings prepared by magnetron sputtering that have shown that the films grown at low temperatures present polycrystalline character and mixed growth mainly along the (111) and (200) planes [14]. From the analysis of the XRD data presented above, using the equation given in the preceding section, we have deduced an average grain size of 9–18 nm along the (111) plane for the films grown at room temperature and different power supplies and of 10–26 nm along the same direction for the films grown at 300 W and different temperatures. These values agree well with those recently reported for similar type of coatings (10–50 nm) [15]. The growth behavior observed here can be explained by the so-called structure zones model [16] where the ratio T_s/T_m (T_s substrate temperature, T_m melting temperature) determines the different growth mechanisms. In the case of nitride transition materials, T_s/T_m ratios between 0.1 and 0.3 (0.13–0.19 in

our case) imply appreciable self-diffusion and the formation of a dense array of fibrous grains separated by more nearly conventional grain boundaries, probably due the occurrence of a coalescence sintering type during growth.

In a different set of experiments, we introduced nitrogen gas in the deposition chamber to study the influence that the addition of this gas during deposition exerts on the structural properties of the NbN films. Figure 2b shows the diffraction patterns recorded from the films grown at 300 W, 553 K and different nitrogen flows. The results obtained make clear that, in all cases, a preferential growth appears along the (200) plane (Fig. 2b). The relative intensity of this diffraction line is so high that makes impossible to distinguish the diffraction lines corresponding to other planes. To determine the polycrystalline character of the film we carried out X-ray diffraction experiments at grazing incidence. Figure 3 shows a representative example. It is clear from Fig. 3 that the films present the same diffraction peaks than the target, confirming their polycrystalline character, although showing a preferential orientation along the (200) plane (texture index, 0.65). The grain sizes deduced for the different grown films along the (200) plane vary from 35 nm ($\Phi = 2$ sscm) to 42 nm ($\Phi = 6$ sscm). These results indicate that incorporation of nitrogen during the fabrication process favors the preferential growth of the δ-NbN phase along the (200) plane.

Previous works on the growth of NbN thin films by different techniques (sputtering, cathodic arc, and reactive methods) [17, 18] have established that the reasons for the variation in texture may depend on factors such as the treatment of the substrate prior coating, the deposition rate [6] the type of substrate and the highly non-equilibrium condition of the plasma sputtering [19]. Furthermore, Bendavid et al. [20] showed that the substrate bias voltage
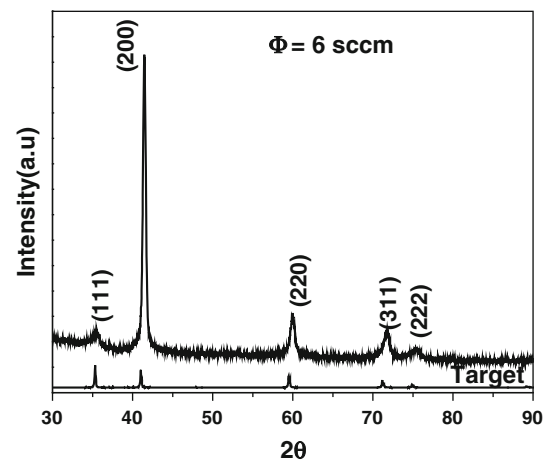

Fig. 3 Grazing angle (2°) XRD pattern recorded from a NbN film grown at 553°K, 300 W, and 6 sccm nitrogen flux. The target XRD pattern is included as reference

also affects the microstructure and preferred orientation. We would also comment that it has been shown [21] that changing the nitrogen flow during the growth of TiN films interchanges the preferred orientation of the films from the [111] direction to the [200] direction.

The incorporation of nitrogen during the deposition process implies changes in the dynamics of the plasma since the increase in the number of nitrogen molecules increases the probability of collisions, promoting a larger number of chemical reactions on the substrate surface. These reactions can be explained using a model of low energy ($\leq$20 eV) ion bombardment during film growth at a T_s/T_m ratio ranging between 0.1 and 0.3 [22, 23]. According to this model, 25 eV are sufficient to cause collisional dissociation of the N_2^+ ions, providing a continuous source of atomic nitrogen. The nitrogen readily chemisorbs on the (200) planes but not on the N-terminated (111) planes This in turn reduces the mean free path of the metal cation on the (200) plane due to capture by the nitrogen atoms, and promotes the formation of a NbNi (i = 1–4) admolecule or islands of adatoms [22, 23]. This can be considered as causing an additional decrease in the (200) surface energy relative to that of the (111) plane. Consequently, the presence of the nitrogen atoms reduces the flux of cations from the (200) to the (111) planes, resulting in the orientation of the growth in the [200] direction.

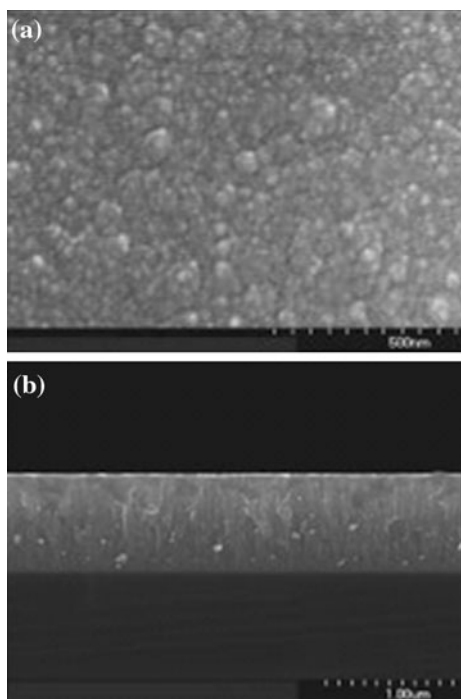The SEM study (Fig. 4) indicates that the grown NbN films present a compact granular structure, with an average grain size of 26 nm, and columnar growth of the type described by Volmer–Weber [24] having an average thickness of 0.7 μm, which implies a deposition rate of 20 nm/min under our experimental conditions. Figure 5 shows the grain size distribution obtained from the SEM observations. The values obtained by SEM correlate well with those calculated by XRD.

The WDS analysis of the films grown at a power of 300 W and a temperature of 553 K is given in Table 1. The results confirm that the films grown under these experimental conditions are stoichiometric. The analysis of films grown under different nitrogen flows did not change substantially.

An XPS analysis of the film deposited at 553 K, N_2 flux of 6 sccm and power of 300 W was carried out in order to study the NbN film surface composition when grown in a N_2 rich environment. The results obtained are shown in Fig. 6a–c. The Nb 3d spectrum (Fig. 6a) shows three different spin–orbit doublets: the most intense one is characterized by a binding energy (BE) of the Nb $3d_{5/2}$ core level of 206.5 eV which is characteristic of Nb_2O_5; the second component appears at a binding energy of the Nb $3d_{5/2}$ core level of 203.6 eV and can be associated to NbN while the third component (BE of the Nb $3d_{5/2}$ core level, 204.8 eV) corresponds, most likely, to the presence of a niobium oxynitride [25, 26]. The N1s spectrum recorded from the above mentioned film is shown in Fig. 6b. It shows three components: a major one at 397.6 eV corresponding to NbN, a second one at 399.3 eV, which we associate to Nb oxynitrides, and a third one at 400.7 eV which might be associated with the presence of molecular N_2.

Finally, Fig. 6c presents the O1s spectrum recorded from the film which shows three contributions: the first one centered at 529.8 eV corresponds to Nb–O bonds in Nb_2O_5
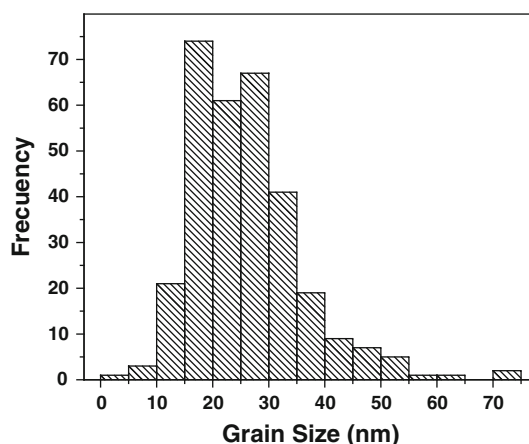

Fig. 4 a Morphology micrograph of a NbN film, b Cross-section micrograph of the NbN film grown at 300 W and 513 K

Fig. 5 Size grain distribution of the NbN film grown at 300 W and 553 K

Table 1 WDS analysis of the NbN thin films grown at 300 W and 553 K

Element (X-ray line)	Weight %	Atomic %
Nb (Lα)	86.8	49.8
N (Kα)	13.2	50.2

[27], a second one at 531.6 eV is characteristic of OH groups and a third one at 532.9 eV might be associated to adsorbed water or C=O bonds.

These results indicate that the last 5 nm of the film (those accessible through XPS) have a complex composition. Nb_2O_5 is, most certainly, the most external phase and must be formed by the oxidation of NbN at some stage of the film fabrication, either in the preparation chamber due to the presence of residual oxygen, or because of fresh film exposure to the lab atmosphere. The Nb oxy-nitride corresponds to a phase located between the most external niobium oxide and the whole NbN film. It is important to point out that very similar XPS results have been obtained in a previous NbN work where the films were prepared without the additional introduction of N_2 [13].

Conclusions

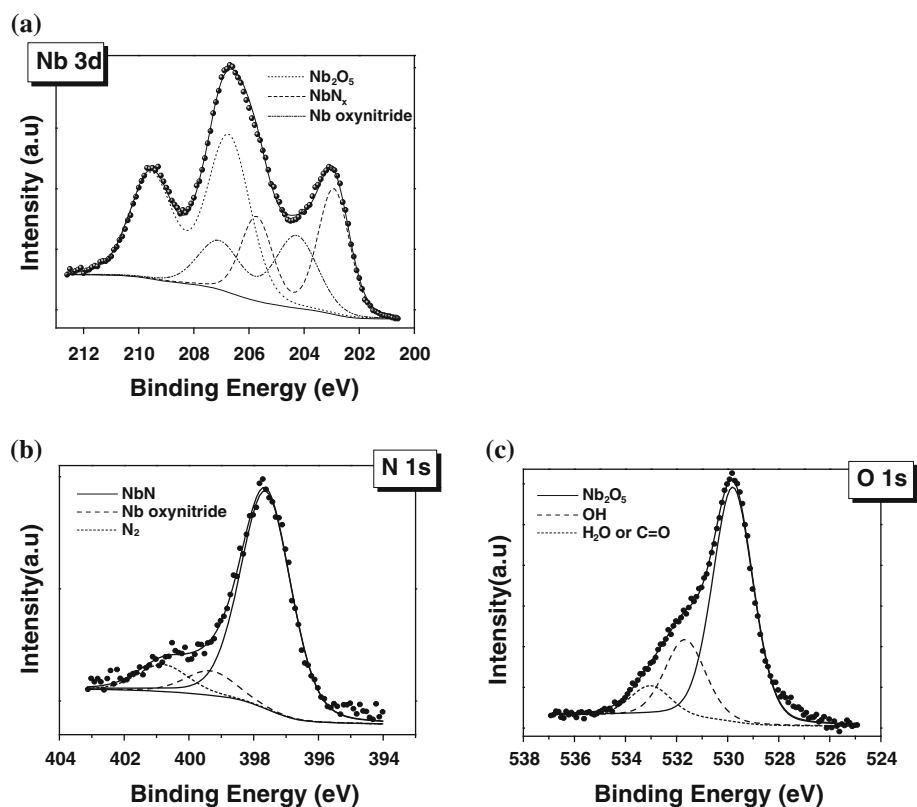The results obtained in this work indicate that during the preparation of NbN films by rf magnetron sputtering the variation of some fabrication parameters such as the power supplied to the target, the substrate temperature or the flux of additional nitrogen gas introduced in the preparation chamber, influence the crystallinity and preferred orientation of the deposited films. In general, the results show that the films copy the target δ-cubic structure and that, with certain fabrication parameters, films grow with nanometer size grain and high texture.

The type of preferential orientation achieved is not the same depending on the variation of one or other fabrication parameter. So, for a power of 300 W and no additional nitrogen, an increase of substrate temperature yields a preferential film growth along (111) plane of the cubic phase δ-NbN, while for a 300 W power, 553 K substrate temperature and additional increase of nitrogen flux preferential orientation of the films along (200) plane is achieved. However, fabrication parameter changes do not significantly affect the surface composition of the deposited films.

References

1. Ishiguro T, Matsushima K, Hamasaki K (1993) J Appl Phys 73:1151
2. Wang Z, Kawakami A, Uzawa Y, Komiyama B (1996) J Appl Phys 79:7837
3. Gotoh Y, Nagao M, Ura T, Tsuji H, Ishikawa J (1999) Nucl Instr Meth Phys Res B 148:925

Fig. 6 XPS spectra recorded from a NbN film grown in a nitrogen-rich atmosphere; **a** Nb 3d spectrum, **b** N1s spectrum, **c** O1s spectrum

4. Jiménez Riobóo RJ, Brien V, Pigeat P (2010) J Mater Sci 45:363. doi:10.1007/s10853-009-3944-3

5. Yu C, Wang S, Tian L, Li T, Xu B (2009) J Mater Sci 44:300. doi:10.1007/s10853-008-3066-3

6. Wong MS, Sproul WD, Chu X, Barnett SA (1993) J Vac Sci Technol A 11:1528

7. Havey KS, Zabinski JS, Walck SD (1997) Thin Solid Films 303:238

8. Alén P, Ritala M, Arstila K, Keinonen J, Leskela M (2005) Thin Solid Films 491:235

9. Yu JH, Park DS, Kim JH, Jeong TS, Youn CJ, Hong KJ (2010) J Mater Sci 45:130. doi:10.1007/s10853-009-3902-0

10. Yucho WM, Venvik HJ, Walmsley JC, Stange M, Ramachandran A, Mathiesen RH, Borg A, Bredesen R, Holmestad R (2009) J Mater Sci 44:4429. doi:10.1007/s10853-009-3671-9

11. Cole M, Podpirka A, Ramanathan S (2009) J Mater Sci 44:5332. doi:10.1007/s10853-009-3538-0

12. Alfonso JE, Torres J, Marco JF (2006) Brazilian J Phys 36:994

13. Alfonso JE, Buitrago J, Torres J, Santos B, Marco JF (2008) Microelectron J 39:1327

14. Olaya JJ, Rodil SE, Mulh S (2008) Thin Solid Films 516:8319

15. Han Z, Hu X, Tian J, Li G, Mingyuan G (2004) Surf Coat Technol 179:188

16. Thorton JA (1974) J Vac Sci Technol 11:666

17. Rutherford KL, Hatto PW, Davies C, Hutchings IM (1996) Surf Coat Technol 86–87:472

18. ZhitoMirsky VN, Grimberg I, Rapport L, Travitzky NA, Boxman RL, Goldsmith S, Raihel A, Lapsker I, Weiss BZ (1998) Thin Solid Films 326:134

19. Chu X, Wong MS, Sproul WD, Rhode SL, Barnett SA (1992) J Vac Sci Technol A 10:1618

20. Bendavid A, Martin PJ, Kinder TJ, Preston EW (2003) Surf Coat Technol 163–164:347

21. Huang J-H, Lau K-W, Yu G-P (2005) Surf Coat Technol 191:17

22. Petrov I, Barna PB (2003) J Vac Sci Technol A 21:S117

23. Gall D, Kodambaca S, Wall MA, Petrov I, Greene JE (2003) J Appl Phys 93:9086

24. Albella JM (ed) (2003) Láminas delgadas y recubrimientos. Preparación y aplicaciones. Biblioteca de Ciencias. Consejo Superior de Investigaciones Científicas (CSIC). Madrid-España

25. Jouve G, Séverac C, Cantacuzène S (1996) Thin Solid Films 287:146

26. Ho SF, Contarini S, Rabalais JW (1987) J Phys Chem 91:4779

27. Garbassi F (1981) J Electron Spectrosc Relat Phenom 22:95